

10-16-2004

Ice Nucleation in Internally Mixed Ammonium Sulfate/Dicarboxylic Acid Particles

Matthew E. Wise

University of Colorado, Boulder, mawise@cu-portland.edu

Rebecca M. Garland

University of Colorado, Boulder

Margaret A. Tolbert

University of Colorado, Boulder

Follow this and additional works at: <http://commons.cu-portland.edu/msfacultyresearch>

 Part of the [Chemistry Commons](#)

Recommended Citation

Wise, Matthew E.; Garland, Rebecca M.; and Tolbert, Margaret A., "Ice Nucleation in Internally Mixed Ammonium Sulfate/Dicarboxylic Acid Particles" (2004). *Faculty Research*. 70.
<http://commons.cu-portland.edu/msfacultyresearch/70>

This Article is brought to you for free and open access by the Math & Science Department at CU Commons. It has been accepted for inclusion in Faculty Research by an authorized administrator of CU Commons. For more information, please contact libraryadmin@cu-portland.edu.

Ice nucleation in internally mixed ammonium sulfate/dicarboxylic acid particles

Matthew E. Wise, Rebecca M. Garland, and Margaret A. Tolbert

Department of Chemistry and Biochemistry and Cooperative Institute for Research in Environmental Sciences (CIRES), University of Colorado, Boulder, Colorado, USA

Received 31 October 2003; revised 14 July 2004; accepted 23 July 2004; published 9 October 2004.

[1] Recent studies have shown that tropospheric sulfate aerosols commonly contain 50% or more by mass organic species. The influence of these organics on the chemical and physical properties of sulfate aerosols is not fully established. Using an aerosol flow tube technique, we have determined ice nucleation temperatures for particles composed of ammonium sulfate and mixtures of ammonium sulfate with a series of dicarboxylic acids. A calibration curve was developed to allow us to convert the freezing temperatures to a saturation ratio required for ice nucleation. At levels detectable by our experimental technique we find that the freezing temperatures and critical ice saturation ratios of each system were identical, for a given water activity of the solution, even though the solutions contained varying fractions of inorganic and organic components. Further experiments showed that the freezing behavior of pure dicarboxylic acid particles was identical to that of the other systems studied if the water activity was identical. Although the apparent freezing temperatures reported here are substantially warmer than those predicted by the water activity based nucleation theory of T. Koop et al., we find that solution water activity defined the freezing conditions for the systems studied

here. *INDEX TERMS*: 0305 Atmospheric Composition and Structure: Aerosols and particles (0345, 4801); 0320 Atmospheric Composition and Structure: Cloud physics and chemistry; 0365 Atmospheric Composition and Structure: Troposphere—composition and chemistry; *KEYWORDS*: homogeneous ice nucleation, ammonium sulfate, dicarboxylic acids

Citation: Wise, M. E., R. M. Garland, and M. A. Tolbert (2004), Ice nucleation in internally mixed ammonium sulfate/dicarboxylic acid particles, *J. Geophys. Res.*, 109, D19203, doi:10.1029/2003JD004313.

1. Introduction

[2] Cirrus clouds play an important role in the Earth's radiation budget because they increase the Earth's albedo while decreasing emission of infrared radiation to space. These opposing effects are thought to cause an overall net warming at the Earth's surface. However, there are large uncertainties in the magnitude of this forcing because, in part, the mechanisms by which cirrus clouds form are not fully understood [*Intergovernmental Panel on Climate Change (IPCC)*, 2001]. Cirrus clouds may also affect heterogeneous chemistry in the upper troposphere as they have been implicated in midlatitude ozone depletion [*Solomon et al.*, 1997]. Therefore the conditions under which cirrus clouds form are essential for modeling the climate and chemistry of the upper troposphere.

[3] It is thought that cirrus clouds form via homogeneous nucleation in the upper troposphere (UT) when the background aerosols cool and become supersaturated with respect to ice. If the correct temperature and relative humidity (RH) conditions are met, these aerosols can homogeneously or heterogeneously nucleate ice to form cirrus cloud particles. Field measurements have shown that background tropospheric aerosols are largely composed of

inorganic species such as ammonium sulfate. Previous laboratory studies [see *Martin*, 2000] as well as thermodynamic models [*Clegg et al.*, 1998a, 1998b; S. L. Clegg et al., aerosol inorganics model, <http://mae.ucdavis.edu/wexler/aim>] have firmly established the deliquescence relative humidity (DRH) and the hygroscopic growth curve of pure ammonium sulfate. These studies also found that fairly low RH conditions are required for the efflorescence of ammonium sulfate particles in the atmosphere. Because of these findings, ammonium sulfate will most likely exist as a solution under many atmospheric conditions. Therefore several studies, using a variety of particle techniques, have been performed to report the conditions necessary for the homogeneous nucleation of ice in ammonium sulfate/water particles [*Bertram et al.*, 2000; *Chen et al.*, 2000; *Cziczo and Abbatt*, 1999; *Hung et al.*, 2002; *Prenni et al.*, 2001b]. Although there is an abundance of aerosol data for ice formation from ammonium sulfate solution aerosol, large discrepancies exist among "apparent" freezing temperatures in these studies. These discrepancies have yet to be reconciled. *Hung and Martin* [2001] hypothesized that one common intrinsic volume nucleation rate function (*J*) is expressed differently in each experiment thus yielding different apparent freezing temperatures. However, *Hung and Martin* [2001] showed that no single *J* function exists that reconciles these experimental results.

[4] A particular difficulty in the determination of J values for aerosol flow tube experiments arises due to vapor phase mass transfer from aqueous particles to interstitial ice particles. This phenomenon greatly contributes to the “onset” of ice formation detected using infrared (IR) spectroscopy and may lead to warmer onset freezing temperatures when compared to other particle techniques. The IR spectroscopic methods used in aerosol flow tube experiments are useful for the determination of the amount of ice formation. However, the potential importance of vapor to ice mass transfer in producing the ice formation event does not allow a simple determination of the fraction of particles nucleating or a nucleation rate. In this paper, we report onset freezing temperatures with the knowledge that vapor to ice mass transfer may contribute to ice events at warmer temperatures than reported by previous research groups.

[5] Experimental uncertainties aside, these studies have focused solely on homogeneous ice nucleation from pure ammonium sulfate. However, there is also evidence that organic material may compose 50% or more of the particle mass [Murphy *et al.*, 1998] in the UT. Rogge *et al.* [1993] identified more than 80 different organic compounds in tropospheric aerosols including water soluble, low molecular weight dicarboxylic acids such as succinic, malonic, and glutaric acids. Recent laboratory studies have determined the DRHs and hygroscopic growth curves of a variety of low molecular weight dicarboxylic acids and multifunctional acids [Braban *et al.*, 2003; Peng *et al.*, 2001; Prenni *et al.*, 2001a; Wise *et al.*, 2003] using both particle and bulk solution techniques. Further laboratory studies and thermodynamic models have determined the DRHs and hygroscopic growth curves of mixed inorganic and organic particles [Ansari and Pandis, 2000; Brooks *et al.*, 2002, 2003; Choi and Chan, 2002a, 2002b; Cruz and Pandis, 2000; Hameri *et al.*, 2002; Ming and Russell, 2002; Prenni *et al.*, 2003; Wise *et al.*, 2003]. However, there is very little data for ice formation from organic and ammonium sulfate/organic solution aerosol.

[6] Koop *et al.* [2000] compiled homogeneous ice nucleation data from supercooled aqueous solution droplets (1–10 μm) containing 18 different types and concentrations of solutes from several published laboratory studies. The solutes dissolved in the aqueous solution droplets included strongly dissociating acids such as sulfuric acid, salts such as ammonium sulfate, and weakly dissociating organics such as glucose. Methods of determining temperatures at which ice homogeneously nucleated from the particles included emulsion and microscope techniques, but did not include freely floating particle techniques such as Fourier transform infrared (FTIR) aerosol measurements. Although there is some spread in the compiled experimental data, Koop *et al.* [2000] showed that the homogeneous nucleation of ice from supercooled aqueous solution droplets depends only on the water activity of the solution and is independent of the type of solute. Therefore, if water activity is known, the temperature at which ice homogeneously nucleates from the particles can be calculated. It is important to note that the model of Koop *et al.* [2000] predicts greater supercooling in ammonium sulfate particles than has been observed in several studies using freely floating particles [Cziczo and Abbatt, 1999; Hung *et al.*, 2002; Prenni *et al.*, 2001b].

[7] Because discrepancies in the conditions required for ice nucleation in particles containing ammonium sulfate from different experimental apparatus have yet to be resolved, the purpose of this paper is to qualitatively test the Koop *et al.* [2000] hypothesis for organics mixed with ammonium sulfate using a FTIR technique which employs freely floating particles. Therefore we have determined the compositions, apparent freezing temperatures, and temperature-dependant critical ice saturation ratios needed to homogeneously nucleate ice in ammonium sulfate/dicarboxylic acid particles in our flow tube setup. The organic compounds studied are glutaric, maleic, and l-malic acid.

2. Experiment

2.1. Flow Tube System

[8] The experimental setup for measuring ice nucleation from internally mixed ammonium sulfate/dicarboxylic acid particles is similar to that used by Prenni *et al.* [2001b] and is shown schematically in Figure 1. During a freezing experiment, aerosol passes through a series of jacketed flow tubes that are cooled with recirculating flows of methanol from Neslab refrigerators. The first series of flow tubes is used to set the composition of the aerosol and will be referred to as the conditioning region. Prior to each experiment, a humidified flow of nitrogen is passed over the conditioning region thus coating the tube walls with ice. The relative humidity in the conditioning region is set by the temperature in this region and is determined using water and ice vapor pressure measurements from Wexler [1976] and Marti and Mauersberger [1993], respectively. If the aerosol is in equilibrium with the water vapor at that temperature, the aerosol will have a well-defined composition and water activity. Particle freezing occurs in the observation tube and is detected using FTIR transmission spectroscopy. The junction between the conditioning tube and the observation tube is termed the transition region, and is cooled (by separate Neslab refrigerators) on one end at the observation temperature and on the other end at the conditioning temperature. Because the temperature drop from the conditioning to the observation region occurs in this transition region, the aerosol has time to reach the observation temperature before being monitored with FTIR spectroscopy.

[9] Submicrometer particles are generated by feeding bulk solutions at 0.3 ml/min into an atomizer (TSI 3076) using a Harvard apparatus syringe pump. After atomization, the particles then pass over a 70 wt % sulfuric acid bath, which reduces gas and condensed phase water, thus preconditioning the aerosol. Using scanning mobility particle size measurements, we have determined that $\sim 10^6$ particles/cm³ with a mean droplet diameter of 0.3 μm and a geometric standard deviation of $\sigma = 1.54$ exit the preconditioning bath. Following the preconditioning bath, the particles pass through the flow tubes at ~ 3.5 L/min. The conditioning region is approximately 4 cm in diameter and 2 m in length, providing a residence time of ~ 45 s. The transition and observation regions are approximately 4 cm in diameter and 75 cm in length, providing a residence time of ~ 16 s. As shown by Prenni *et al.* [2001b], the residence time at 3.5 L/min is long enough for the aerosol to reach equilibrium in the conditioning region and rapid enough for the aerosol

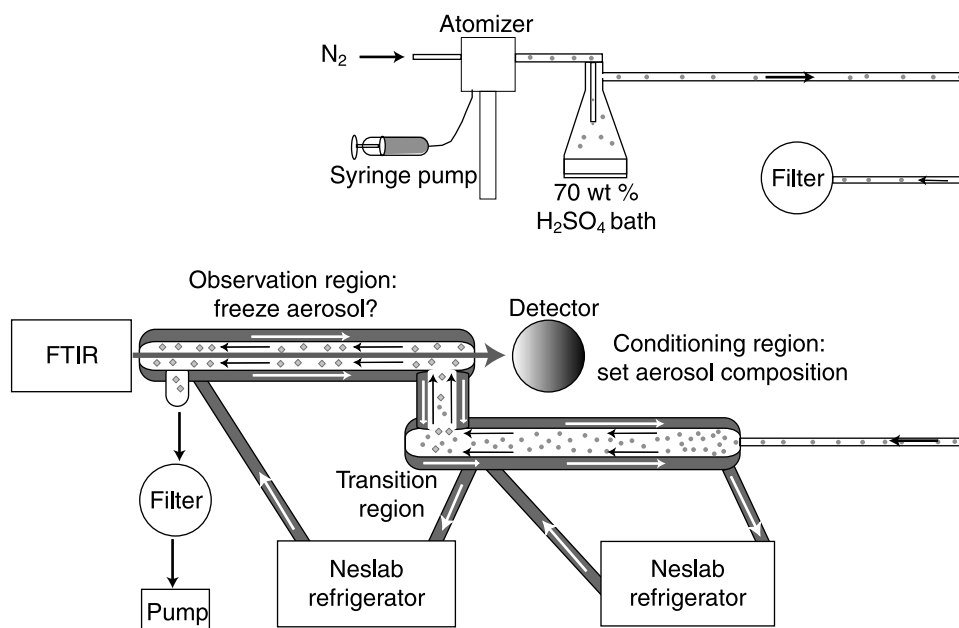


Figure 1. Experimental setup for measuring ice nucleation from ammonium sulfate and internally mixed ammonium sulfate/dicarboxylic acid particles. Submicrometer aerosol is generated using a TSI atomizer. The aerosol composition is then set using a sulfuric acid bath preconditioner and the conditioning region of the flow tubes. Ice nucleation is measured using Fourier transform infrared spectroscopy (FTIR) in the observation region.

to retain its composition in the colder observation region. Because of these conditions, particle composition and water activity are set in the conditioning region. As the temperature is dropped in the observation region, particle composition remains the same; however, particle water activity may change slightly. Therefore the water activity reported in the remainder of this paper is the particle water activity obtained in the conditioning region.

[10] Temperature is measured using thermistors placed at various points in the conditioning and observation regions. Specifically, four thermistors are placed in the observation region (3 in the methanol flow, 1 in the aerosol flow), and 3 thermistors are placed in the conditioning region (2 in the methanol flow, 1 in the aerosol flow). Each thermistor is calibrated against a reference temperature measurement to ± 0.20 K over the temperature range studied and temperature is recorded every 2–3 s during a freezing experiment. The temperature measurements from the thermistors placed in the aerosol flow are averaged for each freezing point measurement. For all experiments, the uncertainty in the temperature measured by the thermistors is always ≤ 0.60 K.

2.2. Aqueous Composition of the Particles

[11] The aqueous composition of pure ammonium sulfate particles in the ice coated conditioning region can be determined using two separate methods. If the aerosol is in equilibrium with the temperature and water vapor in the conditioning region, ammonium sulfate composition can be calculated using the aerosol inorganics model (AIM) [Clegg *et al.*, 1998a, 1998b; S.L. Clegg *et al.*, aerosol inorganics model, <http://mae.ucdavis.edu/wexler/aim>]. Alternatively, ammonium sulfate composition can be determined from the infrared spectra using the composition calibration curve constructed by *Chelf and Martin* [2001]. Specifically, with

the water vapor lines subtracted, the peak area ratio of the integrated water band (1751 cm^{-1} – 1549 cm^{-1}) to the sulfate band (1180 cm^{-1} – 1025 cm^{-1}) is plotted as a function of aqueous ammonium sulfate composition. Therefore, if these peak areas are known, ammonium sulfate composition can be determined.

[12] In aerosols containing both ammonium sulfate and organic compounds, the composition at which each of the solutes is saturated in the presence of one another is termed the “eutonic” composition. As the aerosols absorb and lose water (depending on relative humidity) the water content of the aerosol changes but the solid ammonium sulfate to organic ratio remains the same. Because the solid proportion in the aerosols never changes, we term the mixed systems in this study as “eutonic” systems even though aerosol water content fluctuates as a function of relative humidity. The aqueous composition of the mixed ammonium sulfate/dicarboxylic acid particles in the ice coated conditioning region cannot be determined using the methods previously outlined because the AIM model and the IR calibration curve do not take into account the presence of organics in the aerosol. Since the Kelvin effect is negligible for particles with radii $0.05\text{ }\mu\text{m}$ or larger [Dufour and Defay, 1963], bulk thermodynamics can be used to predict the water uptake and thus composition of aerosol systems. We thus used bulk measurements to determine the composition of the mixed aerosol at a fixed temperature of $\sim -5.75^\circ\text{C}$ in the conditioning region, corresponding to $a_w = 0.946$. Although we also performed freezing experiments in which the conditioning region is set at colder temperatures, thus reducing the water activity and increasing the solute concentration in the particle, we were unable to make bulk measurements of the particle composition because the bulk solutions freeze at lower tube temperatures.

[13] We created bulk precursor saturated solutions (at the eutonic composition) by simultaneously mixing ammonium sulfate and each organic in distilled water according to the solubility data taken from *Brooks et al.* [2002] at -10°C . Approximately 5–10 mL of the bulk precursor solution was placed in a sealed test tube in a liquid nitrogen bath and attached to a mechanically pumped glass line. Once the solution had frozen, the test tube was opened to the evacuated glass line and the gaseous contents pumped away. This procedure was repeated twice to remove all gases from the bulk solution. Once melted, the test tube was placed in $\sim -5.75^{\circ}\text{C}$ temperature controlled bath. After equilibration, the vapor pressure of the sample was measured using a 10 Torr Baratron capacitance manometer (accurate to $\pm 0.15\%$ of the pressure reading). Pure water samples were tested to verify that the measured water vapor pressure agreed with the value calculated using the bath temperature and data from *Wexler* [1976]. It was found that, within error, both values of water vapor pressure agreed. The sample water activity in the mixed solutions was then determined by ratioing the measured sample vapor pressure to the saturation vapor pressure of water.

[14] Simulation of water uptake by the eutonic aerosols was accomplished by adding varying aliquots of water to each of the saturated precursor solutions. After adding water to the saturated solutions, the RH was determined as outlined above. In this way, hygroscopic growth curves at $\sim -5.75^{\circ}\text{C}$ were constructed. Because the accuracy of the capacitance manometer is very high, the uncertainty in the sample temperature ($\pm 0.2^{\circ}\text{C}$) was used to calculate the uncertainty in the water activity measurements which we report to be between 0.010–0.016. The hygroscopic growth curves were then used to determine the aerosol composition at $a_w \sim 0.946$ and a temperature of $\sim -5.75^{\circ}\text{C}$.

2.3. Measuring Ice Crystallization

[15] At the beginning of a freezing experiment, an aerosol infrared spectrum is taken at a temperature well above the freezing temperature to insure that no ice is present in the particles. The temperature of the observation region is then incrementally cooled while keeping the conditioning region at a constant temperature. At each observation temperature, the phase of the aerosol is monitored using FTIR spectroscopy. Near the freezing point of the aerosol, the observation region is cooled in ~ 1 K increments until ice formation is observed in the infrared spectrum (T_{onset}). At the freezing point, several changes occur in the infrared spectrum of the aerosol. The OH-stretching region, which has a maximum at $\sim 3300\text{ cm}^{-1}$ for liquid solutions [*Hung et al.*, 2002] shifts to lower frequencies and the H_2O stretch centered at $\sim 800\text{ cm}^{-1}$ shifts to higher frequencies. Because these changes can be subtle at the onset of particle freezing, each spectrum is subtracted from the previous one as the temperature is incrementally reduced. Using the formalism of *Hung et al.* [2002], the variance in the extinction values of these difference spectra between 690 cm^{-1} and 880 cm^{-1} , weighted by the inverse of the temperature difference between the two spectra, is plotted versus temperature. The freezing temperature is noted by inspection and an increase in the variance between spectra. After the initial freezing point of the aerosol, the observation region is

further cooled in ~ 1 K increments until a maximum in the variance plot is clearly observed (T_{peak}).

[16] As a test of this method of analysis, we also plotted the temperature-normalized variance in the extinction values of each difference spectra between 690 cm^{-1} and 800 cm^{-1} and between 500 cm^{-1} and 1500 cm^{-1} . The freezing temperatures calculated using these different spectral ranges agree with the previous variance analysis between 690 cm^{-1} and 880 cm^{-1} . Therefore we are confident that interferences with the spectral range monitored for aerosol freezing due to the presence of organics is not occurring.

2.4. Experimental Determination of S_{ice}

[17] To determine the critical ice saturation ratios (S_{ice}) needed to homogeneously nucleate ice (at levels detectable by our FTIR method) in mixtures of ammonium sulfate/dicarboxylic acids, the vapor pressure of the particles at the freezing temperature is required. Currently, low-temperature vapor pressure data does not exist for solutions of ammonium sulfate/dicarboxylic acids. Using the water uptake data we obtained from the bulk property measurements on each ammonium sulfate/dicarboxylic acid solution, we made solutions that had a water activity of ~ 0.946 . We then measured the vapor pressure of each solution at a variety of other temperatures ($\sim 0^{\circ}\text{C}$ to $\sim -12^{\circ}\text{C}$) using the method outlined in the previous section. By plotting the natural log of vapor pressure versus inverse temperature for all the eutonic solutions studied, the vapor pressure of each particle at its freezing temperature can be extrapolated and S_{ice} estimated.

3. Results and Discussion

3.1. Low-Temperature Water Uptake of Ammonium Sulfate/Dicarboxylic Acid Particles to Determine Composition

[18] To validate our experimental method for studying water activity and hygroscopic growth of mixed ammonium sulfate and dicarboxylic acid particles, the water uptake curve at -5.78°C was first determined for ammonium sulfate. Figure 2 shows the inverse of the mass fraction solid soluble ($1/\text{mfs}$) versus water activity for ammonium sulfate at and after the deliquescence relative humidity (DRH) in this study as well as predicted values from the AIM model at -5.78°C . The inverse of the mass fraction solid soluble is calculated using equation (1):

$$1/\text{mfs} = 1 + (g_{\text{water}}/g_{\text{solid}}) \quad (1)$$

where g_{water} is the grams of water in solution and g_{solid} is the grams of solid in solution. We measure a relative humidity of 82.2% at -5.78°C for a saturated ammonium sulfate solution, in good agreement with the water activity at the deliquescence point reported at -10°C in bulk studies [*Brooks et al.*, 2002] and in particle studies [*Onasch et al.*, 1999]. Within the experimental error, the water uptake curve we measure by adding various aliquots of water to solid ammonium sulfate agrees well with the predicted values from the AIM model. Figure 3 shows $1/\text{mfs}$ versus water activity for all the eutonic systems in this study at $\sim -5.75^{\circ}\text{C}$. Included in Figure 3 are power law expression fits to each data set of the general form:

$$1/\text{mfs} = y_0 + B(a_w)^C \quad (2)$$

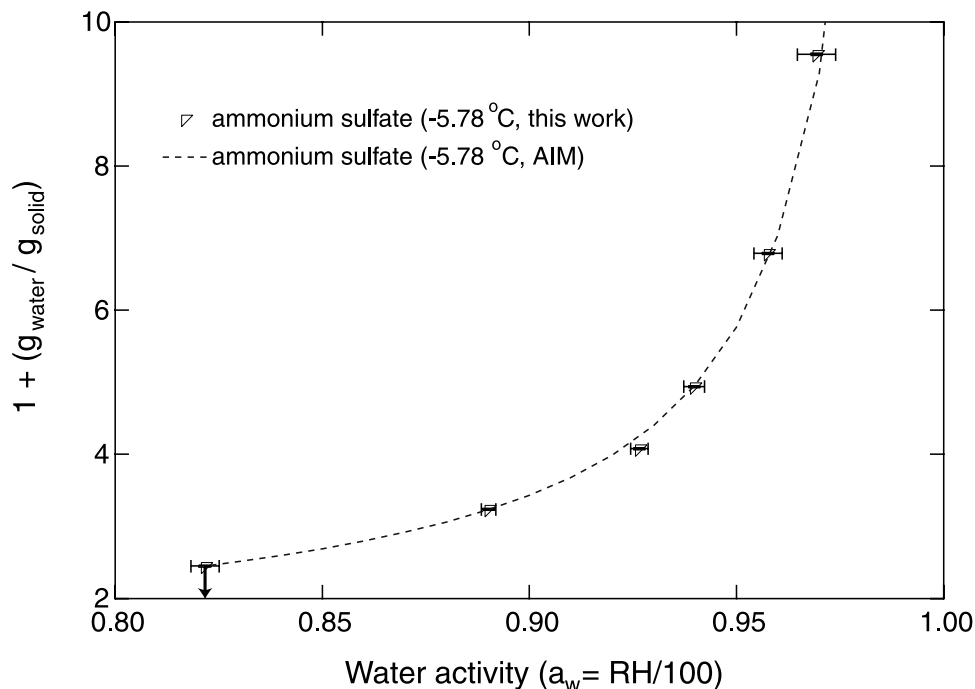


Figure 2. Inverse of the mass fraction solid soluble ($1/mfs$) versus water activity for ammonium sulfate at and after the DRH in this study as well as predicted values from the AIM model at -5.78°C . We measure a DRH of 82.2% at -5.78°C (denoted by a downward arrow) for ammonium sulfate.

where y_0 , B , and C are empirical fitting parameters. This empirical equation satisfactorily fits each data set, and the empirical fitting parameters for each eutonic system are listed in Table 1. Also included in Table 1 is the aerosol composition at one conditioning tube temperature (T_{cond}) in

our aerosol freezing experiments. These compositions were determined using the power law expression fits for each system from the low-temperature bulk water uptake studies at an a_w of ~ 0.946 (shown as horizontal lines in Figure 3). Error in each of the fit coefficients (\pm one standard

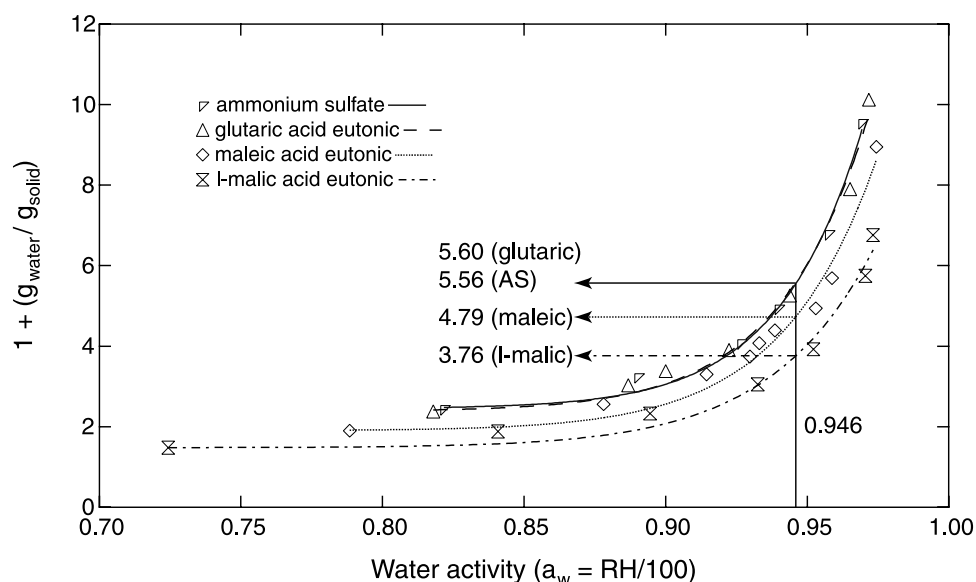


Figure 3. Inverse of the mass fraction solid soluble ($1/mfs$) versus water activity for all the eutonic systems in this study at $\sim -5.75^{\circ}\text{C}$. Each line represents a power law expression fit to each data set with the general form of $1/mfs = y_0 + B(a_w)^C$. This empirical equation satisfactorily fits each data set and the empirical fitting parameters for each system are listed in Table 1. The aerosol composition at the conditioning tube temperature (T_{cond}) in our aerosol freezing experiments are determined using the power law expression fits for each system at an a_w of ~ 0.946 (shown as horizontal lines).

Table 1. Empirical Fitting Parameters for Each Eutonic System and Aerosol Composition at T_{cond}

System	$T_{\text{LTWU}}^{\text{a}}$ °C	Fit Coefficients ^b			$T_{\text{conds}}^{\text{c}}$ °C	Aerosol Composition at $T_{\text{cond}}^{\text{d}}$	
		y_0	B ($\pm 1\sigma$)	C ($\pm 1\sigma$)		wt % Ammonium Sulfate	wt % Organic
Ammonium sulfate	−5.78	2.45	19.3 (± 1.9)	32.9 (± 2.4)	−6.02	18.9 ^{e,f}	
Glutaric acid/ammonium sulfate	−5.68	2.38	17.8 (± 1.7)	30.9 (± 2.5)	−5.81	16.1	2.02
Maleic acid/ammonium sulfate	−5.73	1.90	14.0 (± 1.7)	28.4 (± 2.5)	−5.91	11.4	10.0
l-malic acid/ammonium sulfate	−5.74	1.48	10.2 (± 1.3)	27.0 (± 3.6)	−5.83	8.48	18.5

^aError in temperature measured for the low-temperature bulk water uptake (LTWU) studies is $\pm 0.2^\circ\text{C}$.

^bFit coefficients to the power law expression determined by the LTWU studies, $1/mfs = y_0 + B(a_w)^C$.

^cFor all experiments the uncertainty in the conditioning tube temperature is always ≤ 0.60 K.

^dError in each of the fit coefficients (\pm one standard deviation) as well as the error in the T_{cond} measurement are used to determine the percent error in both ammonium sulfate and organic concentration in the solutions which is always $< 13\%$ of the reported values.

^eWt % ammonium sulfate calculated from the AIM model at -6.02°C model is 19.31 wt %.

^fWt % ammonium sulfate calculated from the IR method at -6.02°C model is 18.35 wt %.

deviation) as well as the error in the T_{cond} measurement are used to determine the percent error in both ammonium sulfate and organic concentration in the solutions which is always $< 13\%$ of the reported values.

3.2. Ice Nucleation in Ammonium Sulfate Particles

[19] Prior to performing freezing experiments on ammonium sulfate/dicarboxylic acid solution particles, we performed freezing experiments on ammonium sulfate solution particles. The impetus for performing these experiments was two fold. First, we wanted to verify that the residence time was long enough for the aerosol to reach equilibrium in the conditioning region and short enough for the aerosol to

retain its composition in the colder observation region. Second, we wanted to compare the conditions necessary for ice nucleation in a pure sulfate aerosol to that of a mixed ammonium sulfate/organic aerosol in the same experimental apparatus. We chose to perform freezing experiments for particles whose composition ranged from less than 20 wt % ammonium sulfate ($a_w \sim 0.946$) to greater than 50 wt % ammonium sulfate ($a_w \sim 0.723$). In this way an atmospherically relevant span of particle compositions were studied.

[20] Figure 4a shows an example of spectral data obtained when aqueous ammonium sulfate particles are cooled from 234.16 K (spectrum 1) to 228.92 K (spectrum 3) in the observation region while the conditioning region is held at a

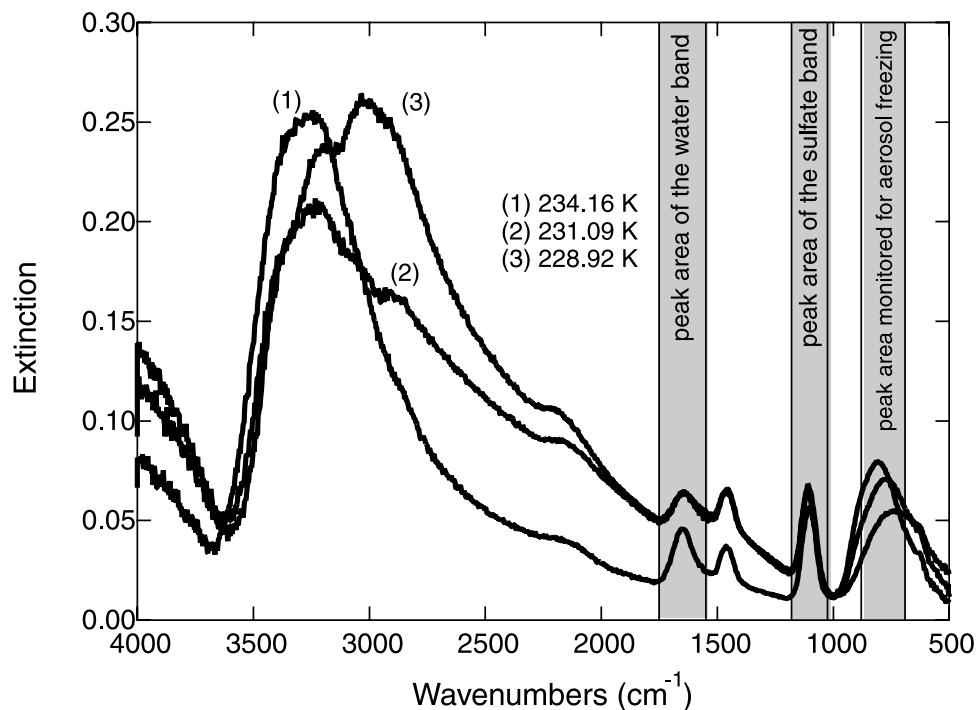


Figure 4a. Spectral data obtained when aqueous ammonium sulfate particles are cooled from 234.16 K (spectrum 1) to 228.92 K (spectrum 3) in the observation region while the conditioning region is held at a constant -6.02°C ($a_w = 0.943$). Ammonium sulfate concentration in the liquid particle at 234.16 K is determined using the AIM model and also by the ratio of the peak area of the integrated water band to the sulfate band. As the temperature is dropped in the aqueous ammonium sulfate particles from 234.16 K to 231.09 K (spectrum 2), the H_2O stretch centered at ~ 800 cm^{-1} shifts to higher frequencies, indicating that some of the aqueous ammonium sulfate particles are frozen. As the temperature is dropped to 228.92 K, other spectral features of ice become increasingly apparent.

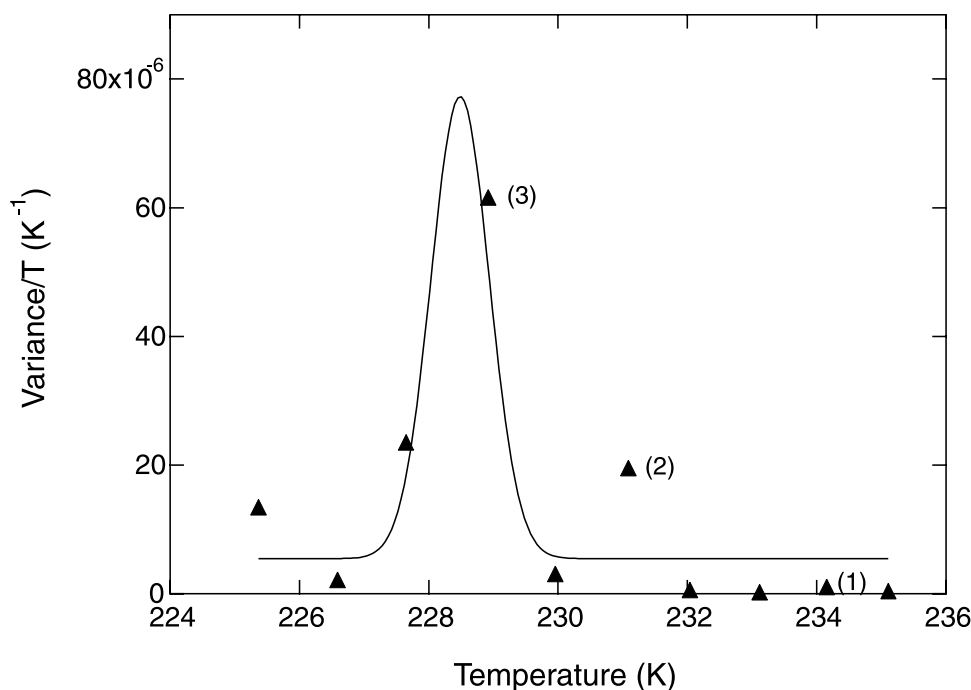


Figure 4b. Variance plot of the entire ammonium sulfate freezing experiment when the conditioning tube is held at -6.02°C (~ 18.4 – 19.3 wt %). The numbered points in Figure 4b refer to the corresponding numbered spectra in Figure 4a. Point 2 is the temperature at which we see the onset of freezing (T_{onset}) in the ammonium sulfate particles. The solid line represents a Gaussian fit to all the freezing point data and the maximum of this empirical fit corresponds to the temperature at which the maximum change in the IR spectra is observed and is denoted as T_{peak} .

constant -6.02°C ($a_w = 0.943$). Indicated on the spectra are the areas in the spectrum that are monitored during a freezing experiment to determine particle composition. Ammonium sulfate concentration in a solution particle is determined by ratioing the peak area of the integrated water band to the sulfate band. At 234.16 K no ice is observed in the infrared spectrum and the ammonium sulfate concentration in the particle (calculated using these peak areas and the calibration of *Chelf and Martin* [2001]) is 18.35 wt %. *Chelf and Martin* [2001] state that the uncertainty in their IR calibration is 0.1 wt % in composition and 0.1 in the peak area ratio. Applying these error criteria to our determination of ammonium sulfate composition, we find that for all experiments, the uncertainty in ammonium sulfate composition calculated using the IR calibration curve method is ≤ 4 wt %. If the aerosol is in equilibrium with the temperature and water vapor in the conditioning region, ammonium sulfate composition can be calculated using the AIM model. The AIM model only takes into account the temperature, and hence the water vapor pressure, in the ice coated conditioning region. The AIM model estimates the ammonium sulfate composition in the particle to be 19.31 wt %. The error associated with this method of determining ammonium sulfate composition arises from the uncertainty in the temperature measured by the thermistors in the conditioning region. It was found that for all experiments, the uncertainty in ammonium sulfate composition calculated using the AIM model is ≤ 2 wt %. Our low-temperature bulk water uptake method leads to an estimated sulfate composition of ~ 18.9 wt %. The difference in particle composition calculated using the three

methods outlined above are within the error of the methods; therefore we are confident that our flow tube system is working correctly.

[21] At the freezing point, several changes occur in the infrared spectrum of the aerosol. One prominent change occurs at the H_2O stretch centered at ~ 800 cm^{-1} , which shifts to higher frequencies as freezing occurs. As the temperature is dropped in the aqueous ammonium sulfate particles from 234.16 K to 231.09 K (spectrum 2), this shift in the H_2O stretch becomes perceptible, designating that some of the aqueous ammonium sulfate particles are frozen. As the temperature is dropped to 228.92 K, the shift at ~ 800 cm^{-1} becomes more pronounced and other spectral features of ice, such as shift of the OH-stretching region at ~ 3300 cm^{-1} , become increasingly apparent.

[22] Because the changes that accompany ice formation in submicron particles can be subtle at the onset of freezing, each spectrum is subtracted from the previous one as the temperature is incrementally reduced. The variance in the extinction values between 690 cm^{-1} and 880 cm^{-1} of these difference spectra, weighted by the inverse of the temperature difference between the two spectra, is plotted versus temperature. The freezing temperature is then noted by inspection and by an increase in the variance between spectra. The variance plot of the entire ammonium sulfate freezing experiment when the conditioning tube is held at -6.02°C (~ 18.4 – 19.3 wt %) is shown in Figure 4b. The numbered points in Figure 4b refer to the corresponding numbered spectra in Figure 4a. Point 2 is the temperature at which we see the onset of freezing (T_{onset}). The solid line in Figure 4b represents a Gaussian fit to the freezing point

Table 2. Compositions, Freezing Temperatures, and Calculated S_{ice} Values for Ammonium Sulfate^a

Conditioned Particle a_w	Composition, wt %		T_{onset}^d K	T_{peak}^d K	Fit Coefficients ^e		S_{ice} at T_{onset}			S_{ice} at T_{peak}		
	AIM ^b	IR ^c			m ($\pm 1\sigma$)	b ($\pm 1\sigma$)	Calibration $P_{H_2O}^f$	Variable AIM a_w^g	Constant AIM a_w^g	Calibration $P_{H_2O}^f$	Variable AIM a_w^g	Constant AIM a_w^g
~ 0.946	19.31	18.35	231.70	229.35	-5.47 (± 0.01)	14.8 (± 0.1)	1.47	1.41	1.40	1.51	1.44	1.43
~ 0.870	34.71	34.57	227.50	222.00				1.35	1.34		1.42	1.41
~ 0.723	51.11	47.12	212.65	211.32				1.29	1.28		1.30	1.30

^aCompositions, freezing temperatures, and S_{ice} values were calculated using an average of two freezing experiments.

^bFor all experiments the uncertainty in ammonium sulfate composition calculated using the AIM model is ≤ 2 wt %.

^cFor all experiments the uncertainty in ammonium sulfate composition calculated using the IR calibration curve method is ≤ 4 wt %.

^dError in T_{onset} and T_{peak} is always ≤ 2 K.

^eFit coefficients to the line determined by the low-temperature bulk studies, $\ln P_{H_2O}/P_o = m(1000/T) + b$ ($R^2 > 0.99$).

^fErrors in the coefficients of equation (4) for each individual system as well as errors in the freezing temperatures were used to calculate error in S_{ice} , which we report to be ≤ 0.10 .

^gErrors in both the condition region temperatures as well the freezing temperatures were used to calculate error in S_{ice} , which we report to be ≤ 0.05 .

data. The maximum of this empirical fit corresponds to the temperature at which the maximum change in the IR spectra is observed and is denoted as T_{peak} . Error associated with the determination of T_{onset} and T_{peak} arises from the uncertainty in the temperature measured by the thermistors in the observation region and the 1 K incremental cooling method outlined in section 2.3. Therefore error in T_{onset} and T_{peak} is always ≤ 2 K.

[23] Table 2 shows our observed T_{onset} and T_{peak} values from ammonium sulfate solution aerosol as well as the particle composition determined by the AIM model and the IR method. The difference in particle composition calculated using the two methods for all particle compositions is within the error of the two methods; therefore we are confident that our reported compositions are accurate.

[24] The ice nucleation data in Table 2 show that lower freezing temperatures occur for more concentrated ammonium sulfate aerosols. However, the water activity based nucleation theory developed by *Koop et al.* [2000] predicts greater supercooling in ammonium sulfate particles when compared to our observed freezing temperatures, especially in the more concentrated aerosols.

[25] A concern in aerosol flow tube experiments is the possibility that solid ammonium sulfate particles are present in the flow tube system. If solid ammonium sulfate particles were present in the observation region, the IR method of calculating solution concentration would give erroneous values because the calibration curve is valid only for the aqueous portion of the aerosol [*Hung et al.*, 2002]. This is not the case as we have clearly shown that the IR method of calculating solution concentration is identical to the AIM method. As a second check to confirm that solid ammonium sulfate was not present in our system, we cooled ammonium sulfate aerosols below the paraelectric to ferroelectric phase transition of 223 K. This phase transition can be seen as distinct changes in the infrared spectrum between 1050 and 1170 cm^{-1} . In all our ammonium sulfate freezing experiments that were carried out to temperatures below 223 K, we did not see a change in the infrared spectrum between 1050 and 1170 cm^{-1} . This indicates the absence of solid ammonium sulfate. Finally, *Cziczo et al.* [1997] notes that the asymmetric 1420 cm^{-1} ammonium peak indicates the presence of solid ammonium sulfate. Again, we did not see this indicator of solid ammonium sulfate in our infrared spectrum. Because we have determined the concentration of ammonium sulfate in the particles using two distinctly

different methods with the same result and because we see no perceptible presence of a phase change in ammonium sulfate and the asymmetric 1420 cm^{-1} peak in our IR spectra, we are confident that the presence of solid ammonium sulfate is not affecting our freezing conditions.

[26] It is not the intent of this study to further establish the temperatures at which various solutions of ammonium sulfate homogeneously nucleate ice. However, what is of particular concern is that freezing temperatures reported in this study differ slightly (warmer nucleation temperatures in more concentrated particles) from freezing temperatures reported by *Prezzi et al.* [2001b]. This is surprising as the freezing measurements presented in this study and in the *Prezzi et al.* [2001b] study come from the same group using the same flow tube apparatus. A secondary concern is that our freezing data differs slightly from previously published freezing data employing freely floating ammonium sulfate particles [e.g., *Bertram et al.*, 2000; *Chen et al.*, 2000; *Cziczo and Abbatt*, 1999; *Hung et al.*, 2002]. Factors such as methods of determining solution concentration, particle size, particle size distributions, residence times, and fraction of particles frozen likely contribute to differences in ammonium sulfate freezing temperatures observed. The literature data has been discussed in detail [*Hung and Martin*, 2001] and the major discrepancies can be resolved by considering the number of freezing events occurring. However, *Hung and Martin* [2001] also found that no volume nucleation rate function exists that can reconcile all experimental results.

[27] Currently, the most widely accepted model for homogeneous ice nucleation in the atmosphere is the *Koop et al.* [2000] model. Upon inspection of Figure 1 of *Koop et al.* [2000], it can be seen at $a_w \sim 0.95$ the spread in the compiled data points is $\sim 10^\circ\text{C}$. Further inspection shows that the spread in compiled data points gets larger as the particles become more concentrated (i.e., a_w decreases). At no ammonium sulfate concentration is the difference in freezing temperatures between this study and the other studies employing freely floating particles greater than the spread in the data used by *Koop et al.* [2000]. Therefore we believe that even though there are differences in our study and other studies employing freely floating particles, they are no greater than that of the currently accepted model for homogeneous ice nucleation.

[28] The ammonium sulfate freezing data can be used to determine the humidity conditions necessary for ice forma-

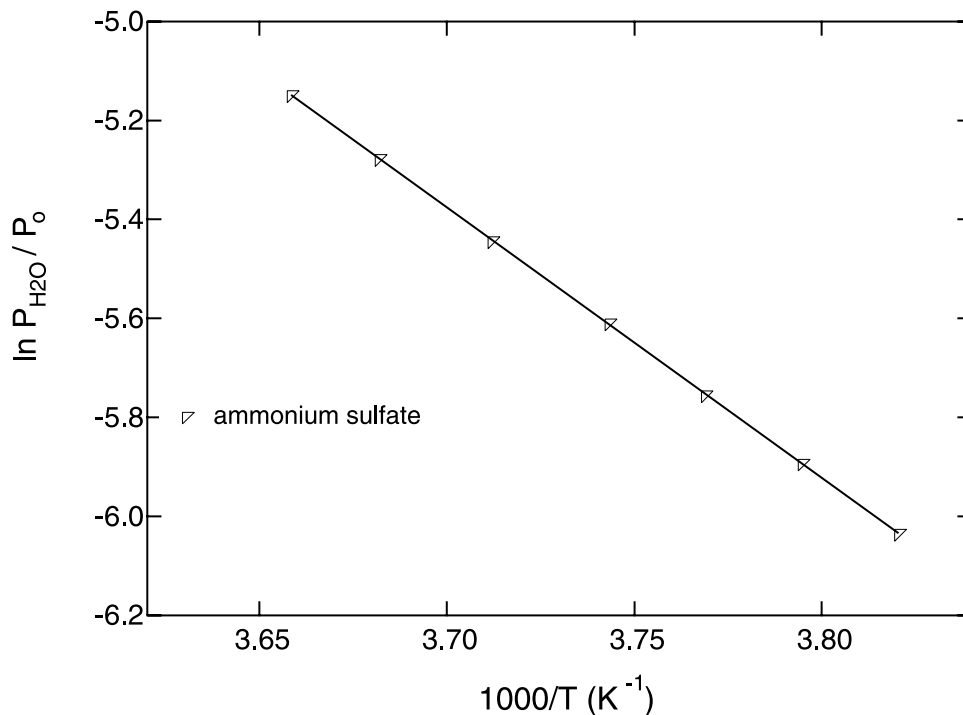


Figure 5. Natural log of solution vapor pressure versus the inverse in temperature for the ~ 19 wt % ammonium sulfate solution. A straight line can be fit through the data with the general form of $\ln P_{\text{H}_2\text{O}}/P_o = m(1000/T) + b$. The coefficients of this linear fit are listed in Table 2.

tion. A parameter widely used in cloud microphysical models is the temperature-dependent critical ice saturation ratio, S_{ice} , which is defined as:

$$S_{\text{ice}} = P_{\text{H}_2\text{O}}/P(T, \text{ice}) \quad (3)$$

where $P_{\text{H}_2\text{O}}$ is the aerosol water vapor pressure at the freezing temperature and $P(T, \text{ice})$ is the vapor pressure of water over ice at the same temperature. To determine S_{ice} , the water vapor pressure of the ammonium sulfate particles at the freezing temperature is required.

[29] Three different methods can be used to determine water vapor pressures of ammonium sulfate particles at the freezing temperatures in our experiments. The first method utilizes the water uptake data we obtained from the bulk property measurements of ammonium sulfate (section 3.1). Using this data, we made ammonium sulfate solutions that had a water activity of ~ 0.946 . We then measured the vapor pressure of each solution at a variety of other temperatures. By plotting the natural log of vapor pressure versus inverse temperature for all the ammonium sulfate solutions studied, the vapor pressure of each particle at its freezing temperature can be extrapolated and S_{ice} estimated. Because the bulk property measurements could only be carried out on solutions that had a water activity of ~ 0.946 , this method was used only for ~ 19 wt % ammonium sulfate particles. Figure 5 shows the natural log of solution vapor pressure versus the inverse in temperature for the ~ 19 wt % ammonium sulfate solution. A straight line can be fit through the data with the form:

$$\ln P_{\text{H}_2\text{O}}/P_o = m(1000/T) + b \quad (4)$$

where $P_{\text{H}_2\text{O}}$ is the solution vapor pressure in atm, $P_o = 1$ atm, m is the slope of the line, T is the temperature of the solution in Kelvin, and b is the y intercept of the line. The coefficients of this linear fit ($R^2 > 0.99$) are listed in Table 2.

[30] The final two methods utilize the AIM model to determine ammonium sulfate particle vapor pressure at the freezing temperature. Particle water activity, which changes slightly due to the temperature difference between the conditioning region and the observation region, can be calculated using the AIM model by assuming a set particle composition. The solution vapor pressure at the freezing temperature, $P_{\text{H}_2\text{O}}$, can then be calculated using the following relation:

$$P_{\text{H}_2\text{O}} = (a_w)(P_{\text{sat}}) \quad (5)$$

where a_w is the particle water activity at the observation region temperature and P_{sat} is the saturation vapor pressure of liquid water at the observation region temperature. Alternatively, particle vapor pressure can be calculated using the AIM model by assuming that the change in particle water activity from the conditioning region to the observation region is small enough that it can be ignored. Therefore a_w in equation (5) is calculated at the conditioning tube temperature.

[31] Table 2 lists S_{ice} values calculated at our onset freezing temperatures as well as our peak freezing temperatures for each of the methods described above. Using the calibration curve method, S_{ice} was calculated to be 1.47 and 1.51 for ammonium sulfate at T_{onset} and T_{peak} , respectively. For this method, errors in the coefficients of equation (4) (\pm one standard deviation) as well as errors in the freezing

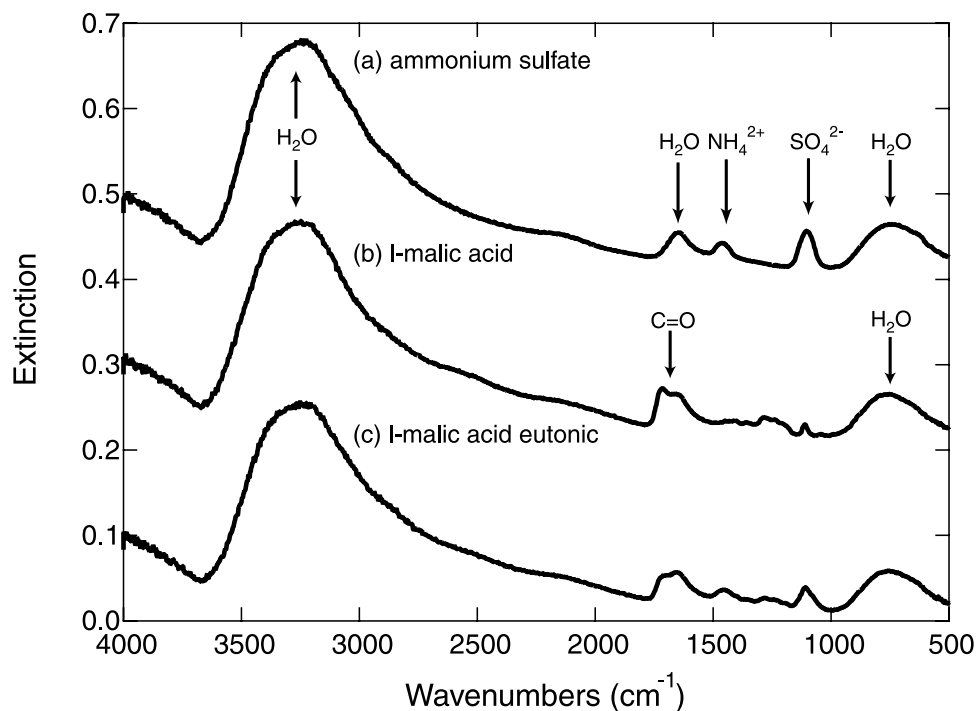


Figure 6. Infrared spectra of (a) ammonium sulfate, (b) l-malic acid, and (c) l-malic acid/ammonium sulfate eutonic solution, each with water activities of ~ 0.946 . All spectra were obtained at $T_{\text{obs}} \sim 233$ K, with spectral features due to gas phase water subtracted. Characteristic peaks of ammonium sulfate and l-malic acid are indicated on the spectra.

temperatures were used to calculate error in S_{ice} , which we report to be ≤ 0.10 . S_{ice} values calculated using the AIM model assuming a variable particle water activity agree very well with S_{ice} values calculated assuming a constant particle water activity both at T_{onset} and T_{peak} . For these two methods, errors in both the condition region temperature as well as the freezing temperatures were used to calculate error in S_{ice} , which we report to be ≤ 0.05 . Because S_{ice} values for ammonium sulfate calculated using vapor pressures from equation (4) and using the AIM models are within error, we feel that each of the three methods of calculating S_{ice} for the ammonium sulfate solutions are good approximations and are interchangeable.

3.3. Ice Nucleation in Ammonium Sulfate/Dicarboxylic Acid Particles

[32] Figure 6 shows infrared spectra of ammonium sulfate (curve a), l-malic acid (curve b), and l-malic acid/ammonium sulfate eutonic solution (curve c), each with water activities of ~ 0.946 . All spectra were obtained at $T_{\text{obs}} \sim 233$ K, with spectral features due to gas phase water subtracted. A characteristic peak of the ammonium ion is clearly present in the ammonium sulfate spectrum at ~ 1460 cm^{-1} as well as the sulfate ion at ~ 1100 cm^{-1} . Because the ammonium sulfate solution aerosol is fairly dilute at $a_w \sim 0.946$, the remaining ammonium ion peaks at ~ 3335 – 3030 cm^{-1} are obscured by liquid phase water bands. A characteristic peak of a dicarboxylic acid at ~ 1715 cm^{-1} , due to the C=O stretching vibration, is present in the l-malic acid spectrum as well as in the l-malic acid/ammonium sulfate eutonic solution spectrum. Also present in the l-malic acid eutonic spectrum are

peaks due to ammonium sulfate. Qualitatively, these reference spectra not only show that we have a atomized a homogeneous eutonic solution aerosol, but also the ratios of l-malic acid peak heights to sulfate peak heights reflect the composition of aerosol we obtained using our low-temperature water uptake data. It is also important to note that the relative peak heights of the water bands in each aerosol are nearly the same indicating that each aerosol has approximately the same water content.

[33] Figure 7a shows an example of spectral data when aqueous l-malic acid/ammonium sulfate eutonic particles are cooled from 232.49 K (spectrum 1) to 230.29 K (spectrum 3) in the observation region while the conditioning region is held at a constant -5.83°C ($a_w = 0.945$). At 232.49 K no ice is observed in the infrared spectrum; however, as the observation tube temperature is lowered to 231.29 K spectral features of ice begin to appear indicating the onset of aerosol freezing. As the temperature is dropped to 230.29 K, other spectral features of ice become increasingly apparent. The variance plot of the entire l-malic acid/ammonium sulfate eutonic freezing experiment when the conditioning tube is held at -5.83°C is shown in Figure 7b. The numbered points in Figure 7b refer to the corresponding numbered spectra in Figure 7a. Point 2 is the temperature at which we see the onset of freezing (T_{onset}) and the maximum in the Gaussian fit to the data points corresponds to the temperature at which the maximum change in the IR spectra is observed (T_{peak}). Values of T_{onset} and T_{peak} for aerosols with $a_w \sim 0.946$ containing dicarboxylic acids are listed in Table 3.

[34] To determine the temperature dependant critical ice saturation ratios needed to homogeneously nucleate ice in

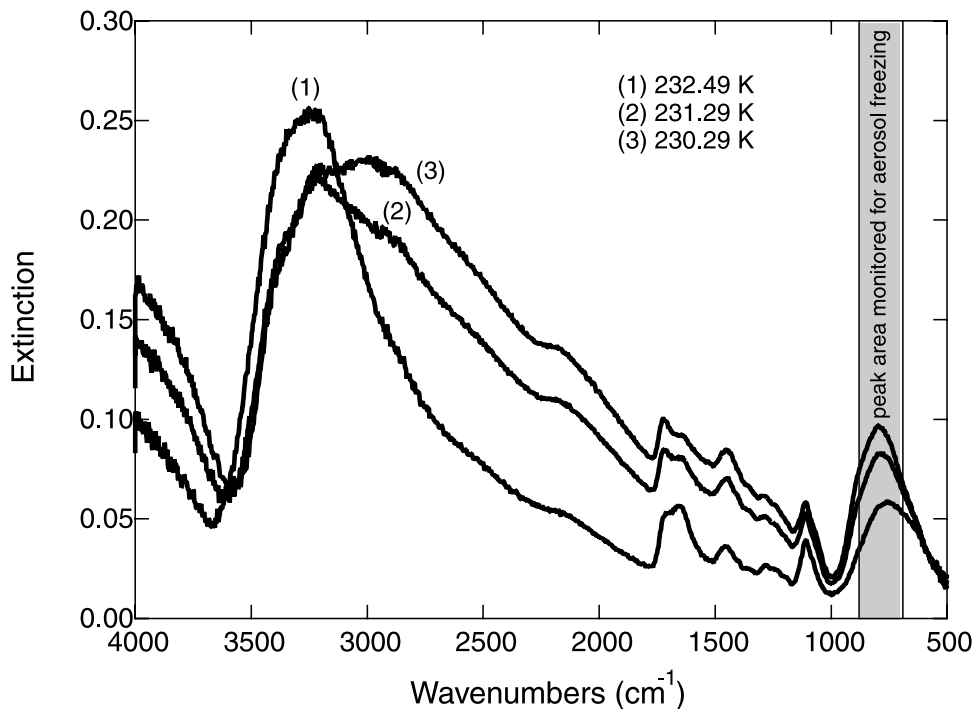


Figure 7a. Spectral data obtained when aqueous l-malic acid/ammonium sulfate eutonic particles are cooled from 232.49 K (spectrum 1) to 230.29 K (spectrum 3) in the observation region while the conditioning region is held at a constant -5.83°C ($a_w = 0.945$). At 232.49 K, no ice is observed in the infrared spectrum; however, as the observation tube temperature is lowered to 231.29 K, spectral features of ice begin to appear, indicating the onset of aerosol freezing. As the temperature is dropped to 230.29 K, all other spectral features of ice become increasingly apparent.

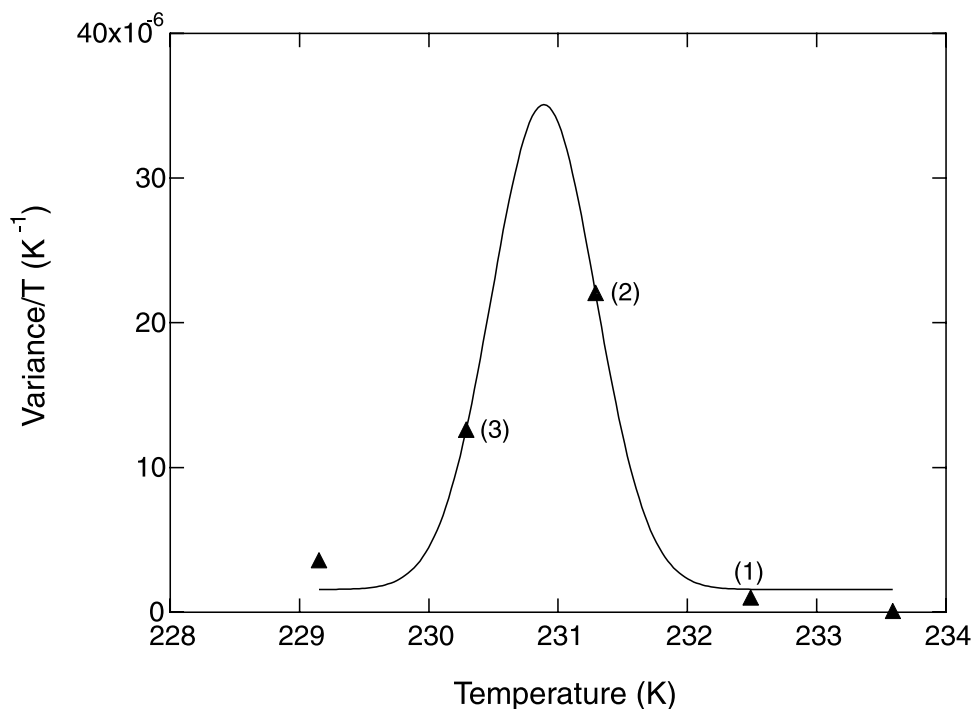


Figure 7b. Variance plot of the entire l-malic acid/ammonium sulfate eutonic freezing experiment when the conditioning tube is held at -5.83°C . The numbered points in Figure 7b refer to the corresponding numbered spectra in Figure 7a. Point 2 is the temperature at which we see the onset of freezing (T_{onset}) and the maximum in the Gaussian fit to the data points corresponds to the temperature at which the maximum change in the IR spectra is observed (T_{peak}).

Table 3. Freezing Temperatures and Calculated S_{ice} Values for Ammonium Sulfate and Mixed Ammonium Sulfate/Dicarboxylic Acid Particles With $a_w \sim 0.946$

System	T_{onset} , ^a K	T_{peak} , ^a K	Fit Coefficients ^b		S_{ice} at T_{onset}		S_{ice} at T_{peak}	
			m ($\pm 1\sigma$)	b ($\pm 1\sigma$)	Calibration P_{H_2O} ^c	Constant a_w ^d	Calibration P_{H_2O} ^c	Constant a_w ^d
<i>Pure Species in Water</i>								
Ammonium sulfate	231.70 ^e	229.35 ^e	-5.47 (± 0.01)	14.8 (± 0.1)	1.47 ^e	1.40 ^e	1.51 ^e	1.43 ^e
l-malic acid	232.08					1.40		
<i>Eutonic Mixtures in Water</i>								
Glutaric acid/ammonium sulfate	230.90 ^e	227.05	-5.46 (± 0.01)	14.8 (± 0.1)	1.50 ^e	1.41 ^e	1.57	1.47
Maleic acid/ammonium sulfate	230.63 ^e	228.10	-5.44 (± 0.03)	14.7 (± 0.1)	1.52 ^e	1.42 ^e	1.57	1.45
l-malic acid/ammonium sulfate	231.30 ^e	230.48 ^e	-5.45 (± 0.01)	14.8 (± 0.1)	1.49 ^e	1.41 ^e	1.50 ^e	1.42 ^e

^aError in T_{onset} and T_{peak} is always ≤ 2 K.

^bFit coefficients to the line determined by the low temperature bulk studies, $\ln P_{H_2O}/P_o = m(1000/T) + b$ ($R^2 > 0.99$).

^cErrors in the coefficients of equation (4) (\pm one standard deviation) for each individual system as well as errors in the freezing temperatures were used to calculate error in S_{ice} , which we report to be ≤ 0.10 .

^dErrors in both the condition region temperatures as well the freezing temperatures were used to calculate error in S_{ice} , which we report to be ≤ 0.05 .

^eAverage of two separate freezing experiments.

mixtures of ammonium sulfate/dicarboxylic acids, the vapor pressure of the particles at the freezing temperature is required. Using the water uptake data we obtained from the bulk property measurements on each ammonium sulfate/dicarboxylic acid solution (section 3.1), we mixed new solutions that had a water activity of ~ 0.946 . We then measured the vapor pressure of each solution at a variety of temperatures, with the lowest temperature being 1 K above the temperature at which the bulk solution froze. Figure 8 shows the natural log of solution vapor pressure versus the inverse in temperature of the ammonium sulfate/dicarboxylic acid eutonic solutions. The coefficients of the linear fits ($R^2 > 0.99$) to each ammonium sulfate/dicarboxylic acid

system with $a_w \sim 0.946$ are included in Table 3. Table 3 also includes corresponding S_{ice} values calculated using extrapolated vapor pressures from equation (4) and using the AIM model assuming a constant water activity. Because S_{ice} values for ammonium sulfate calculated using vapor pressures from equation (4) and using the AIM model are within error, we feel that both methods of calculating S_{ice} for the ammonium sulfate/dicarboxylic acid solutions are good approximations.

[35] Within error, each dicarboxylic acid/ammonium sulfate solution homogeneously nucleates ice at the same temperature. Further, because the vapor pressures for all the solutions are similar, each mixed ammonium sulfate/

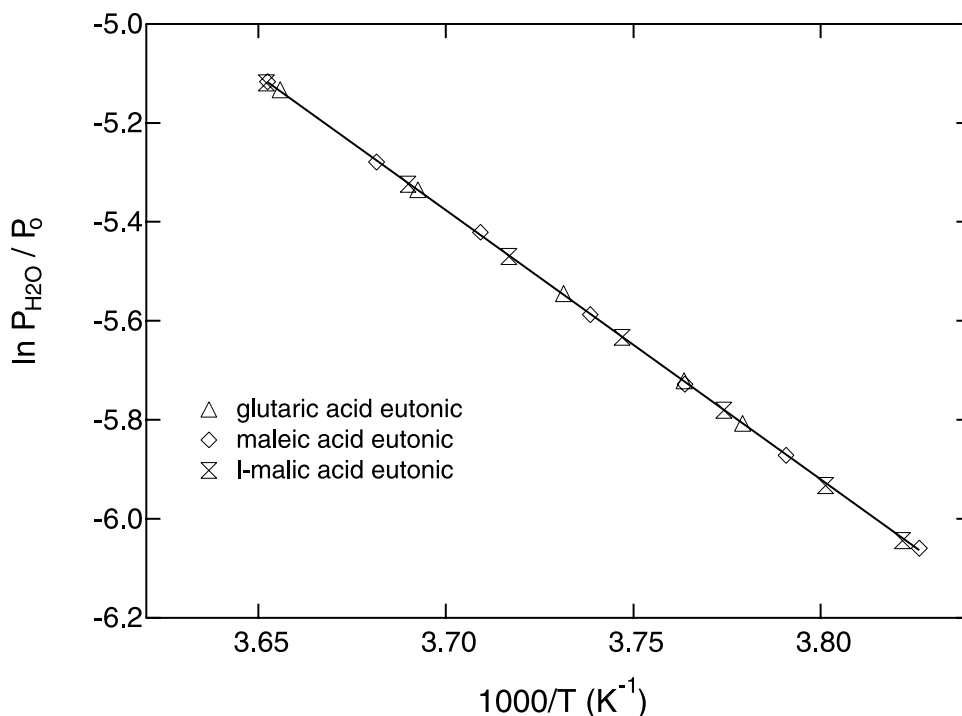


Figure 8. Natural log of solution vapor pressure versus the inverse in temperature for ammonium sulfate and each of the ammonium sulfate/dicarboxylic acid eutonic solutions. A straight line can be fit through the data for each of the solutions studied with the general form of $\ln P_{H_2O}/P_o = m(1000/T) + b$. The coefficients of the linear fits to each individual system are listed in Table 3.

Table 4. Freezing Temperatures and Calculated S_{ice} Values for Ammonium Sulfate, Dicarboxylic Acid, and Mixed Ammonium Sulfate/Dicarboxylic Acid Particles Assuming Constant $a_w = \sim 0.870$ and 0.723

System	$a_w = \sim 0.870$				$a_w = \sim 0.723$			
	T_{onset} , ^a K	S_{ice} at T_{onset} ^b	T_{peak} , ^a K	S_{ice} at T_{peak} ^b	T_{onset} , ^a K	S_{ice} at T_{onset} ^b	T_{peak} , ^a K	S_{ice} at T_{peak} ^b
<i>Pure Species in Water</i>								
Ammonium sulfate	227.50 ^c	1.34 ^c	222.00 ^c	1.41 ^c	212.65 ^c	1.28 ^c	211.32 ^c	1.30 ^c
Glutaric acid	227.46	1.34	223.32	1.40				
Maleic acid	228.09	1.33	223.92	1.38				
l-malic acid	229.97	1.31						
<i>Eutonic Mixtures in Water</i>								
Glutaric acid/ammonium sulfate					213.62	1.27	209.95	1.31
Maleic acid/ammonium sulfate					211.34	1.30	210.58	1.30
l-malic acid/ammonium sulfate	227.79	1.34			212.92	1.28	212.92	1.28

^aError in T_{onset} and T_{peak} is always ≤ 2 K.

^bErrors in both the condition region temperatures as well the freezing temperatures were used to calculate error in S_{ice} , which we report to be ≤ 0.05 .

^cAverage of two separate freezing experiments.

dicarboxylic acid solution nucleated ice at the same S_{ice} for a given a_w . Initially, these results were surprising because each solution has different water uptake characteristics and thus different compositions at the time of freezing. However, *Koop et al.* [2000] show from experimental data that the homogeneous nucleation of ice from supercooled aqueous solutions is solely dependant on its water activity and is independent of the nature of the dissolved solute. Our freezing data qualitatively corroborates this study at least for solutions of ammonium sulfate/dicarboxylic acids at the compositions and temperatures studied. However, as stated earlier, our actual freezing temperatures are substantially warmer than predicted by *Koop et al.* [2000].

[36] We also performed a freezing experiment for particles with $a_w = \sim 0.946$ containing only l-malic acid to determine if pure dicarboxylic acid particles would show similar behavior for homogeneous ice nucleation as ammonium sulfate. The temperature at the onset of freezing is included in Table 3. It was found that the particles homogeneously nucleate ice at the same conditions as that of ammonium sulfate solution aerosol. Because we did not perform low-temperature bulk water uptake studies for pure l-malic acid, we could not determine S_{ice} for this system using the calibration curve method. However, S_{ice} was determined using the AIM model with the assumption of constant water activity. This experiment illustrates that pure dicarboxylic acid particles show similar behavior for homogeneous ice nucleation as ammonium sulfate solution particles if water activity is equal.

[37] Because *Prezzi et al.* [2001a] showed that ice nucleation from organic aerosol was not as effective as ice nucleation from sulfate solution particles (particularly at lower temperatures), we performed additional freezing experiments with the conditioning tube held at $\sim -14.5^\circ\text{C}$ ($a_w = 0.870$), and $\sim -33.7^\circ\text{C}$ ($a_w = 0.723$). Because of the reduced water vapor pressure in the conditioning region, the particles are substantially more concentrated. Therefore colder temperatures are required for homogeneous ice nucleation in the particles and the temperature regime in which *Prezzi et al.* [2001a] show inhibited ice nucleation can be studied. The results of these studies are presented in Table 4. It was found that, in all cases, the particles homogeneously nucleated ice at the same temperature as that of ammonium sulfate solution aerosol with the same

water activity. Because we did not perform low-temperature bulk water uptake studies for any of the solution at the lower conditioning tube temperatures (the bulk solutions froze), we could not determine S_{ice} for these systems using the calibration curve method. However, S_{ice} was determined using the AIM model with the assumption of constant water activity. These experiments further illustrate our conclusion that solutions of ammonium sulfate/dicarboxylic acids show similar behavior for homogeneous ice nucleation as ammonium sulfate solution particles if water activity is equal.

4. Atmospheric Implications

[38] Recently, simultaneous measurements of the concentration and composition of free tropospheric aerosol particles capable of inducing ice formation in cirrus clouds were reported [*DeMott et al.*, 2003]. This study showed that the homogeneous freezing of background sulfate aerosols was impeded if they contained internally mixed organic components. This finding is in qualitative agreement with the *Prezzi et al.* [2001a] study that showed ice nucleation from organic/water solution particles is not as effective as ice nucleation from sulfate solution particles, particularly at lower temperatures. However, this conclusion is in apparent contradiction to the *Koop et al.* [2000] study, which finds that the homogeneous nucleation of ice from supercooled aqueous solutions is solely dependant on its water activity and is independent of the nature of the dissolved solute. It is also in apparent contradiction with the current work where we show mixtures of ammonium sulfate with dicarboxylic acids freeze at the same temperature as pure ammonium sulfate. However, *DeMott et al.* [2003] did not specify the mixing state or the identity of the organic compounds in their aerosols. Therefore investigating the water uptake and ice activity of other mixed organic/inorganic particles at a variety of temperature and RH conditions is needed. In particular it has been suggested that nonwater soluble organic compounds may form a coating onto ammonium sulfate, which may hinder water uptake [*Ellison et al.*, 1999].

[39] **Acknowledgments.** This research was supported by the Biological and Environmental Research Program (BER), U.S. Department of Energy, grant DE-FG03-01ER63096. M.E.W. would like to thank Jonathan

Abbatt, Daniel Cziczo, Hui-Ming Hung, Scot Martin, and Anthony Prenni for helpful input during the development of this manuscript. M.E.W. would also like to thank the NASA-ESS Fellowship Program for funding.

References

- Ansari, A. S., and S. N. Pandis (2000), Water absorption by secondary organic aerosol and its effect on inorganic aerosol behavior, *Environ. Sci. Technol.*, *34*(1), 71–77.
- Bertram, A. K., T. Koop, L. T. Molina, and M. J. Molina (2000), Ice formation in $(\text{NH}_4)_2\text{SO}_4\text{-H}_2\text{O}$ particles, *J. Phys. Chem. A*, *104*, 584–588.
- Braban, C. F., M. F. Carroll, S. A. Styler, and J. P. D. Abbatt (2003), Phase transitions of malonic and oxalic acid aerosols, *J. Phys. Chem. A*, *107*, 6594–6602.
- Brooks, S. D., M. E. Wise, M. Cushing, and M. A. Tolbert (2002), Deliquescence behavior of organic/ammonium sulfate aerosol, *Geophys. Res. Lett.*, *29*(19), 1917, doi:10.1029/2002GL014733.
- Brooks, S. D., R. M. Garland, M. E. Wise, A. J. Prenni, M. Cushing, E. Hewitt, and M. A. Tolbert (2003), Phase changes in internally mixed maleic acid/ammonium sulfate aerosols, *J. Geophys. Res.*, *108*(D15), 4487, doi:10.1029/2002JD003204.
- Chelf, J. H., and S. T. Martin (2001), Homogeneous ice nucleation in aqueous ammonium sulfate aerosol particles, *J. Geophys. Res.*, *106*(D3), 1215–1226.
- Chen, Y., P. J. DeMott, S. J. Kreidenweis, D. C. Rogers, and D. E. Sherman (2000), Ice formation by sulfate and sulfuric acid aerosol particles under upper tropospheric conditions, *J. Atmos. Sci.*, *57*, 3752–3766.
- Choi, M. Y., and C. K. Chan (2002a), Continuous measurements of the water activities of aqueous droplets of water-soluble organic compounds, *J. Phys. Chem. A*, *106*, 4566–4572.
- Choi, M. Y., and C. K. Chan (2002b), The effects of organic species on the hygroscopic behaviors of inorganic aerosols, *Environ. Sci. Technol.*, *36*, 2422–2428, doi:10.1021/es0113293.
- Clegg, S. L., P. Brimblecombe, and A. S. Wexler (1998a), A thermodynamic model of the system $\text{H}^+\text{-NH}_4^+\text{-SO}_4^{2-}\text{-NO}_3^-\text{-H}_2\text{O}$ at tropospheric temperatures, *J. Phys. Chem. A*, *102*, 2137–2154.
- Clegg, S. L., P. Brimblecombe, and A. S. Wexler (1998b), A thermodynamic model of the system $\text{H}^+\text{-NH}_4^+\text{-Na}^+\text{-SO}_4^{2-}\text{-NO}_3^-\text{-Cl}^-\text{-H}_2\text{O}$ at 298.15 K, *J. Phys. Chem. A*, *102*, 2155–2171.
- Cruz, C. N., and S. N. Pandis (2000), Deliquescence and hygroscopic growth of mixed inorganic-organic atmospheric aerosol, *Environ. Sci. Technol.*, *34*(20), 4313–4319.
- Cziczo, D. J., and J. P. D. Abbatt (1999), Deliquescence, efflorescence, and supercooling of ammonium sulfate aerosols at low temperature: Implications for cirrus cloud formation and aerosol phase in the atmosphere, *J. Geophys. Res.*, *104*(D11), 13,781–13,790.
- Cziczo, D. J., J. H. Nowak, J. H. Hu, and J. P. D. Abbatt (1997), Infrared spectroscopy of model tropospheric aerosols as a function of relative humidity: Observation of deliquescence and crystallization, *J. Geophys. Res.*, *102*(D15), 18,843–18,850.
- DeMott, P. J., D. J. Cziczo, A. J. Prenni, D. M. Murphy, S. M. Kreidenweis, D. S. Thomson, R. Borys, and D. C. Rogers (2003), Measurements of the concentration and composition of nuclei for cirrus formation, *Proc. Natl. Acad. Sci. U. S. A.*, *100*(25), 14,655–14,660.
- Dufour, L., and R. Defay (1963), *Thermodynamics of Clouds*, 255 pp., Academic, San Diego, Calif.
- Ellison, G. B., A. F. Tuck, and V. Vaida (1999), Atmospheric processing of organic aerosols, *J. Geophys. Res.*, *104*(D9), 11,633–11,641.
- Hameri, K., R. Charlson, and H. Hansson (2002), Hygroscopic properties of mixed ammonium sulfate and carboxylic acid particles, *AIChE J.*, *48*(6), 1309–1316.
- Hung, H., and S. Martin (2001), Apparent freezing temperatures modeled for several experimental apparatus, *J. Geophys. Res.*, *106*(D17), 20,379–20,394.
- Hung, H., A. Malinowski, and S. T. Martin (2002), Ice nucleation kinetics of aerosols containing aqueous and solid ammonium sulfate particles, *J. Phys. Chem. A*, *106*, 293–306.
- Intergovernmental Panel on Climate Change (2001), *Climate Change 2001: The Scientific Basis*, 944 pp., Cambridge Univ. Press, New York.
- Koop, T., B. Luo, A. Tsias, and T. Peter (2000), Water activity as the determinant for homogeneous ice nucleation in aqueous solutions, *Nature*, *406*, 611–612.
- Marti, J., and K. Mauersberger (1993), A survey and new measurements of ice vapor pressure at temperatures between 170 and 250 K, *Geophys. Res. Lett.*, *20*(5), 363–366.
- Martin, S. T. (2000), Phase transitions of aqueous atmospheric particles, *Chem. Rev.*, *100*(9), 3403–3454.
- Ming, Y., and L. Russell (2002), Thermodynamic equilibrium of organic-electrolyte mixtures in aerosol particles, *AIChE J.*, *48*(6), 1331–1348.
- Murphy, D. M., D. S. Thomson, and M. J. Mahoney (1998), In-situ measurements of organics, meteoric material, mercury, and other elements in aerosols at 5 to 19 kilometers, *Science*, *282*, 1664–1669.
- Onasch, T. B., R. L. Siefert, S. D. Brooks, A. J. Prenni, B. Murray, M. A. Wilson, and M. A. Tolbert (1999), Infrared spectroscopic study of the deliquescence and efflorescence of ammonium sulfate aerosol as a function of temperature, *J. Geophys. Res.*, *104*(D17), 21,317–21,326.
- Peng, C., M. N. Chan, and C. K. Chan (2001), The hygroscopic properties of dicarboxylic and multifunctional acids: Measurements and UNIFAC predictions, *Environ. Sci. Technol.*, *35*, 4495–4501.
- Prenni, A. J., P. J. DeMott, S. M. Kreidenweis, D. E. Sherman, L. M. Russell, and Y. Ming (2001a), The effects of low molecular weight dicarboxylic acids on cloud formation, *J. Phys. Chem. A*, *105*, 11,240–11,248.
- Prenni, A. J., M. E. Wise, S. D. Brooks, and M. A. Tolbert (2001b), Ice nucleation in sulfuric acid and ammonium sulfate particles, *J. Geophys. Res.*, *106*(D3), 3037–3044.
- Prenni, A. J., P. J. De Mott, and S. M. Kreidenweis (2003), Water uptake of internally mixed particles containing ammonium sulfate and dicarboxylic acids, *Atmos. Environ.*, *37*(30), 4243–4251.
- Rogge, W. F., M. A. Mazurek, L. M. Hildemann, G. R. Cass, and B. R. T. Simoneit (1993), Quantification of urban organic aerosols at a molecular level: Identification, abundance and seasonal variation, *Atmos. Environ., Part A*, *8*(27), 1309–1330.
- Solomon, S., S. Borrmann, R. R. Garcia, R. Portmann, L. Thomason, L. R. Poole, D. Winker, and M. P. McCormick (1997), Heterogeneous chlorine chemistry in the tropopause region, *J. Geophys. Res.*, *102*, 21,411–21,429.
- Wexler, A. (1976), Vapor pressure formulation for water in the range 0 to 100 C. A revision, *J. Res. Natl. Bur. Stand. U.S., Sect. A*, *73*(5), 493–495.
- Wise, M. E., J. D. Surratt, D. B. Curtis, J. E. Shilling, and M. A. Tolbert (2003), Hygroscopic growth of ammonium sulfate/dicarboxylic acids, *J. Geophys. Res.*, *108*(D20), 4638, doi:10.1029/2003JD003775.

R. M. Garland, M. A. Tolbert, and M. E. Wise, Department of Chemistry and Biochemistry and Cooperative Institute for Research in Environmental Sciences (CIRES), University of Colorado, Boulder, CO 80309, USA. (matthew.wise@asu.edu)